Trans-endocytosis of intact IL-15Rα–IL-15 complex from presenting cells into NK cells favors signaling for proliferation

Olga M. Anton[a,b,1], Mary E. Peterson[a], Michael J. Hollander[c], David W. Dorward[d], Gunjan Arora[a], Javier Traba[e], Sumati Rajagopalan[a], Erik L. Snapp[f], K. Christopher Garcia[c], Thomas A. Waldmann[b,1,2], and Eric O. Long[a,1,2]

[a]Laboratory of Immunogenetics, National Institute of Allergy and Infectious Diseases, National Institutes of Health, Rockville, MD 20892; [b]Lymphoid Malignancies Branch, Center for Cancer Research, National Cancer Institute, National Institutes of Health, Bethesda, MD 20892; [c]Department of Molecular and Cellular Physiology, Stanford University School of Medicine, Stanford, CA 94305; [d]Microscopy Unit, Research Technologies Branch, Rocky Mountain Laboratories, National Institute of Allergy and Infectious Diseases, National Institutes of Health, Hamilton, MT 59840; [e]Cardiovascular Branch, National Heart, Lung and Blood Institute, National Institutes of Health, Bethesda, MD 20892; and [f]Howard Hughes Medical Institute, Janelia Research Campus, Ashburn, VA 20147

Contributed by Thomas A. Waldmann, November 12, 2019 (sent for review July 8, 2019; reviewed by Thomas R. Malek and Kimberly S. Schluns)

Interleukin 15 (IL-15) is an essential cytokine for the survival and proliferation of natural killer (NK) cells. IL-15 activates signaling by the β and common γ (γ_c) chain heterodimer of the IL-2 receptor through *trans*-presentation by cells expressing IL-15 bound to the α chain of the IL-15 receptor (IL-15Rα). We show here that membrane-associated IL-15Rα–IL-15 complexes are transferred from presenting cells to NK cells through *trans*-endocytosis and contribute to the phosphorylation of ribosomal protein S6 and NK cell proliferation. NK cell interaction with soluble or surface-bound IL-15Rα–IL-15 complex resulted in Stat5 phosphorylation and NK cell survival at a concentration or density of the complex much lower than required to stimulate S6 phosphorylation. Despite this efficient response, Stat5 phosphorylation was reduced after inhibition of metalloprotease-induced IL-15Rα–IL-15 shedding from *trans*-presenting cells, whereas S6 phosphorylation was unaffected. Conversely, inhibition of *trans*-endocytosis by silencing of the small GTPase TC21 or expression of a dominant-negative TC21 reduced S6 phosphorylation but not Stat5 phosphorylation. Thus, *trans*-endocytosis of membrane-associated IL-15Rα–IL-15 provides a mode of regulating NK cells that is not afforded to IL-2 and is distinct from activation by soluble IL-15. These results may explain the strict IL-15 dependence of NK cells and illustrate how the cellular compartment in which receptor–ligand interaction occurs can influence functional outcome.

cytokine | IL-15 | natural killer | signaling

The cytokine interleukin (IL)-15 is crucial for natural killer (NK) cell development, survival, and proliferation (1, 2). The IL-15 receptor (IL-15R) consists of 3 subunits: the α chain, unique to IL-15R; the β chain, shared with IL-2R; and the common γ (γ_c) chain, shared with the receptors for IL-2, IL-4, IL-7, IL-9, and IL-21 (3). Accordingly, NK cells do not develop in mice lacking either IL-15 or any of the 3 IL-15R subunits (4–9). Despite their similarity, IL-15R has properties that are not shared with IL-2R. IL-15Rα has a very high affinity for IL-15 (K_d = 50 pM), whereas IL-2Rα binds IL-2 with a K_d of 10 nM. IL-15Rα and IL-15 are coexpressed in the same cells and exported to the plasma membrane as a complex, with IL-15Rα acting as a chaperone for IL-15 (10–12). Therefore, IL-15 is usually presented in *trans* by cells expressing the IL-15Rα–IL-15 complex, such as stromal cells and dendritic cells (DCs), to cells that express the β-γ_c chains, such as T cells and NK cells (10). Consistent with this, adoptively transferred NK cells lacking the IL-15Rα gene survive in normal mice but not in IL-15Rα–deficient mice (13, 14). Signal transduction from the β-γ_c chains activates multiple pathways, including a pathway that leads to a transcriptional response and cell survival through JAK1/3-dependent phosphorylation of Stat5 (15) and another pathway that activates cell proliferation through PI-3K–Akt–mTOR–dependent phosphorylation of the ribosomal protein S6 by the p70-S6 kinase (16–18).

Trans-presentation of IL-15, resulting in β-γ_c–induced signals in the receiving cell, could occur in several ways. The simplest way is direct contact at the immunologic synapse of membrane-associated IL-15Rα–IL-15 with the β-γ_c signaling complex. An interesting aspect of this interaction is the potential for regulation by other receptor–ligand interactions occurring at the synapse, such as NK cell inhibitory receptors binding to the major histocompatibility complex (MHC) (19). Interaction of NK cells with DC results in the formation of an immunologic synapse with characteristics of both activating and inhibitory synapses, which has been called a regulatory synapse (20–22). As soluble IL-15Rα–IL-15 complex is found in the circulation (23), presumably through proteolytic cleavage from the plasma membrane (24, 25), *trans*-presentation may also occur through release of a soluble IL-15Rα–IL-15 complex. Cleavage of IL-15Rα–IL-15 at the immunologic synapse would be an efficient way to release soluble ligand in the vicinity of its receptor. A third possibility is that the entire

Significance

Interleukin 15 (IL-15) is essential for natural killer (NK) cell survival and proliferation. The IL-15 receptor consists of 3 subunits: the α chain and the β and common γ (γ_c) chains, which are shared with the IL-2 receptor. NK cells express the β-γ_c chains and are activated in *trans* by cells presenting IL-15 bound to IL-15Rα, such as dendritic cells. We show here that the release of soluble IL-15Rα–IL-15 complex from presenting cells contributes to efficient signaling for NK cell survival, whereas uptake of the entire membrane-associated-IL-15Rα–IL-15 complex from presenting cells into NK cells contributes to proliferation. Thus, outcomes are dictated not only by signal strength, but also by location where IL-15 *trans*-presentation occurs in NK cells.

Author contributions: O.M.A. and E.O.L. designed research; O.M.A., M.E.P., M.J.H., D.W.D., G.A., and J.T. performed research; E.L.S. and K.C.G. contributed new reagents/analytic tools; O.M.A., E.L.S., T.A.W., and E.O.L. analyzed data; O.M.A., S.R., T.A.W., and E.O.L. wrote the paper; and K.C.G., T.A.W., and E.O.L. provided supervision and acquired funding.

Reviewers: T.R.M., University of Miami; and K.S.S., The University of Texas MD Anderson Cancer Center.

The authors declare no competing interest.

[1]To whom correspondence may be addressed. Email: olga.antonhurtado@nih.gov, tawald@helix.nih.gov, or eLong@nih.gov.

[2]T.A.W. and E.O.L. contributed equally to this work.

This article contains supporting information online at https://www.pnas.org/lookup/suppl/doi:10.1073/pnas.1911678117/-/DCSupplemental.

First published December 23, 2019.

membrane-associated IL-15Rα–IL-15 receptor is *trans*-endocytosed into β-γ_c– expressing cells. In this case, signaling by β-γ_c would occur in endosomes that have engulfed a vesicle taken from a *trans*-presenting cell carrying IL-15Rα–IL-15.

In this study, we found that IL-15Rα expressed by DCs is internalized by NK cells on *trans*-presentation, and that the IL-15Rα–IL-15 receptor complex colocalizes with the IL-2Rβ chain in intracellular NK cell compartments. Inhibition of matrix metalloproteases (MMPs) to prevent shedding of IL-15Rα–IL-15 did not reduce the *trans*-endocytosis of intact IL-15Rα and activation of ribosomal protein S6 kinase. In contrast, inhibition of MMPs blocked release of the extracellular domain of IL-15Rα and reduced the phosphorylation of Stat5. Silencing of the small GTPase TC21, which promotes *trans*-endocytosis of MHC into T cells (26), inhibited S6 phosphorylation, but not Stat5 phosphorylation, in NK cells. These results support the view that signals for survival of NK cells and signals leading to proliferation are not only dictated by the amount of IL-15Rα–IL-15, but can also be preferentially regulated according to the form of the IL-15Rα–IL-15 complex and the location where it meets IL-2Rβ-γ_c in NK cells.

Results

Transfer of Membrane-Associated and Soluble IL-15Rα from *Trans*-Presenting Cells to NK Cells. IL-15Rα tagged at its C-terminal cytoplasmic tail with mCherry (Fig. 1*A*) and transfected into 721.221 cells (221–IL-15Rα-Cherry) was used to test whether IL-15Rα is transferred into primary NK cells during *trans*-presentation (Fig. 1*A* and *SI Appendix*, Fig. S1*A*). First, the functionality of 221–IL-15Rα-Cherry cells was tested by IL-15 loading (Fig. 1*B*) and stimulation of primary NK cell proliferation (Fig. 1*C*). Cherry signal was detected in NK cells by flow cytometry after mixing with 221–IL-15Rα-Cherry cells (Fig. 1*D*). Consistent with *trans*-endocytosis of intact, membrane-associated IL-15–IL-15Rα-Cherry complex (*SI Appendix*, Fig. S1*B*), its uptake by NK cells was not sensitive to the broad MMP inhibitor GM6001 (Fig. 1*D*). In contrast, shedding of IL-15Rα from 221–IL-15Rα cells after mixing with NK cells was reduced in the presence of GM6001 (*SI Appendix*, Fig. S1*C*).

A second form of IL-15Rα was engineered to test whether soluble IL-15Rα, released by cleavage of the extracellular domain, is also transferred to NK cells (*SI Appendix*, Fig. S1*B*). IL-15Rα was tagged at its N-terminal extracellular domain with Venus (Fig. 1*E*) and transfected into 721.221 cells (221–Venus-IL-15Rα) (*SI Appendix*, Fig. S1*A*). The crystal structure of the complete α–IL-15–β–γ_c receptor complex showed that the α chain N terminus is exposed and points away from the rest of the complex (27), suggesting that a fluorescent protein tag at the N terminus might not impair receptor function. The functionality of 221–Venus-IL-15Rα cells was shown by IL-15 loading (Fig. 1*F*) and by stimulation of primary NK cell proliferation (Fig. 1*G*). The proliferation of primary NK cells was equally effective as that promoted by 221–IL-15Rα-mCherry loaded with exogenous IL-15 (Fig. 1 *C* and *G*). Transfer of Venus-IL-15Rα to primary unstimulated NK cells after mixing with 221–Venus-IL-15Rα cells for 60 min was observed by flow cytometry (Fig. 1*H*). Transfer of IL-15Rα from *trans*-presenting 221 cells to NK cells was more efficient with 221–Venus-IL-15Rα cells than with 221–IL-15Rα-Cherry cells, even though both cells expressed similar levels of IL-15Rα (*SI Appendix*, Fig. S1*A*) and bound a similar amount of IL-15 (Fig. 1 *B* and *F*). Note that Venus-IL-15Rα would be detected in NK cells after transfer of either soluble or *trans*-endocytosed Venus–IL-15Rα–IL-15 complex. These results suggest that soluble Venus–IL-15Rα shed after cleavage by proteases at the plasma membrane contributes to IL-15Rα uptake by NK cells.

To test the possibility of Venus-IL-15Rα transfer due to shedding of the IL-15Rα–IL-15 complex (*SI Appendix*, Fig. S1*B*), we performed cell mixing experiments in the presence of the MMP inhibitor GM6001. Inhibition of IL-15Rα–IL-15 shedding by GM6001 was confirmed by enzyme-linked immunosorbent assay (*SI Appendix*, Fig. S1*C*). In contrast to the *trans*-endocytosis of intact, membrane-associated IL-15–IL-15Rα-Cherry into NK cells, which was not sensitive to MMP inhibition (Fig. 1*D*), transfer of Venus–IL-15Rα to NK cells was partially inhibited by GM6001, consistent with transfer of soluble Venus-IL-15Rα in addition to *trans*-endocytosis of intact Venus-IL-15Rα (Fig. 1*H*). These results show that the IL-15Rα–IL-15 complex can be transferred from *trans*-presenting cells to NK cells as both a transmembrane protein and a soluble receptor.

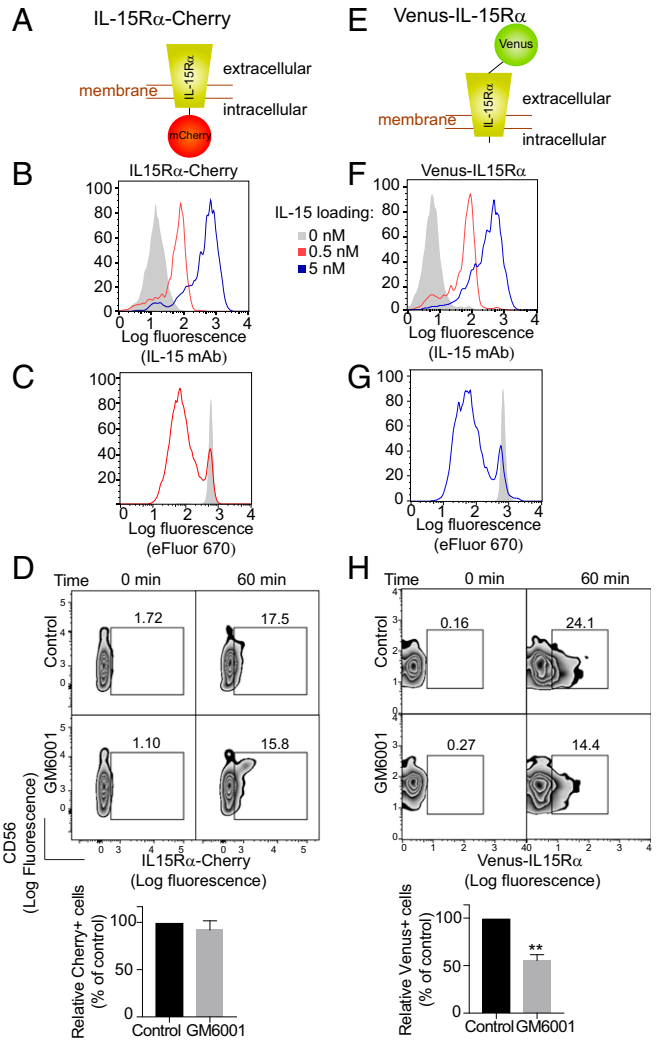

Fig. 1. Transfer of membrane-associated IL-15Rα from *trans*-presenting cells to NK cells. (*A*) Schematic of the IL-15Rα-mCherry construct. (*B*) 221–IL-15Rα-mCherry cells were loaded with the indicated concentrations of IL-15 for 20 min, washed, and stained with an antibody to IL-15 and a secondary antibody coupled to PE. The control histogram (shaded) represents staining of cells not loaded with IL-15. (*C*) Proliferation of NK cells labeled with eFluor 670 and incubated with IL-15–loaded 221–IL-15Rα-mCherry cells (red) for 5 d. The shaded histogram represents NK cells incubated with 221–IL-15Rα-mCherry cells not loaded with IL-15. (*D*) 221–IL-15Rα-Cherry cells were preloaded with 5 nM IL-15 and incubated with primary human NK cells in the absence or presence of 0.4 μg/mL GM6001. Transfer of IL-15Rα-mCherry to NK cells was measured by flow cytometry. A representative experiment is shown. Bar graphs show the mean and SEM of 3 independent experiments relative to the control, untreated cells. (*E*) Schematic of the Venus-IL-15Rα construct. (*F*) 221–Venus-IL-15Rα cells treated as in *B*. (*G*) Proliferation of NK cells labeled with eFluor 670 and incubated with 221–Venus-IL-15Rα cells as in *C*. (*H*) 221–Venus-IL-15Rα cells were treated as in *D*. Transfer of Venus-IL-15Rα to the NK cells was measured by flow cytometry. Statistical analysis was performed using a 2-tailed *t* test. $^{**}P < 0.01$.

Transfer of IL-15Rα from *Trans*-Presenting DCs to Intracellular Compartments in NK Cells. Primary human DCs were transfected with IL-15Rα-mCherry and incubated 24 h later with exogenous IL-15 for 30 min. After incubation with autologous NK cells for 30 min, samples were examined by confocal microscopy. IL-15Rα-mCherry accumulated at the edges of DC–NK cell immunologic synapses (Fig. 2*A*), as observed earlier at synapses of NK cells with 221–IL-15Rα cells (19). A similar distribution was observed after staining fixed cells with an Ab to IL-15 (Fig. 2*A*). Measurements at and away from cell contacts showed that IL-15Rα was ∼1.9 times more concentrated at DC–NK cell synapses compared with an equivalent area of membrane not in contact with NK cells (Fig. 2*B*). A 3D reconstruction of a synapse showed that IL-15Rα and IL-15 accumulated at the periphery of DC–NK cell synapses (Fig. 2 *C* and *D*). After incubation of IL-15Rα-mCherry$^+$ DCs with primary NK cells for 1 h, we could observe the presence of IL-15Rα-mCherry as puncta inside NK cells (Fig. 2*E*). These intracellular compartments partially overlapped with MHC class II compartments (Fig. 2*E*). Of all of the NK cells found in conjugates with DCs after fixation, 54 ± 15% of them showed an intracellular IL-15Rα-mCherry signal (Fig. 2*F*).

We examined the compartments into which IL-15Rα had been internalized in NK cells during IL-15 *trans*-presentation by transmission electron microscopy (TEM). 221–Venus-IL-15Rα cells were loaded with exogenous IL-15 and conjugated with primary NK cells for 30 min. After fixation and permeabilization, cells were incubated with a primary polyclonal anti-GFP antibody, followed by a secondary antibody coupled to horseradish peroxidase (HRP) to detect Venus-IL-15Rα after chromogenic reaction with DAB substrate. Dark staining occurred at sites of contact between 221–Venus-IL-15Rα and NK cells (Fig. 3*A*), and in vesicles inside NK cells (Fig. 3*B*). HRP$^+$ intracellular vesicles were found within a membrane-delimited compartment (Fig. 3*C*), consistent only with *trans*-endocytosis of a fragment of the plasma membrane of *trans*-presenting cells and not with endocytosis of soluble IL-15Rα–IL-15 complex (*SI Appendix*, Fig. S1*B*). *Trans*-endocytic vesicles containing HRP$^+$ Venus-IL-15Rα were also observed in primary NK cells after conjugation with autologous DC transiently transfected with Venus-IL-15Rα (Fig. 3*D*). These results suggest that NK cells capture a piece of the plasma membrane of *trans*-presenting cells and endocytose it once it has been released as a vesicle (*SI Appendix*, Fig. S1*B*).

Colocalization of *Trans*-Endocytosed IL-15Rα–IL-15 Complex with IL-2Rβ in NK Cells. To test whether IL-15Rα acquired by NK cells through *trans*-presentation could be functional, we performed colocalization experiments. The crystal structure of the α–IL-15–β–γ_c receptor complex showed that the N termini of the 3 receptor subunits were exposed and pointing away from one another (27). Therefore, we tagged IL-2Rβ at the N terminus with Cerulean and expressed it in NKL cells (NKL–oxCerulean-IL-2Rβ). As Cerulean is sensitive to the oxidizing milieu in the lumen

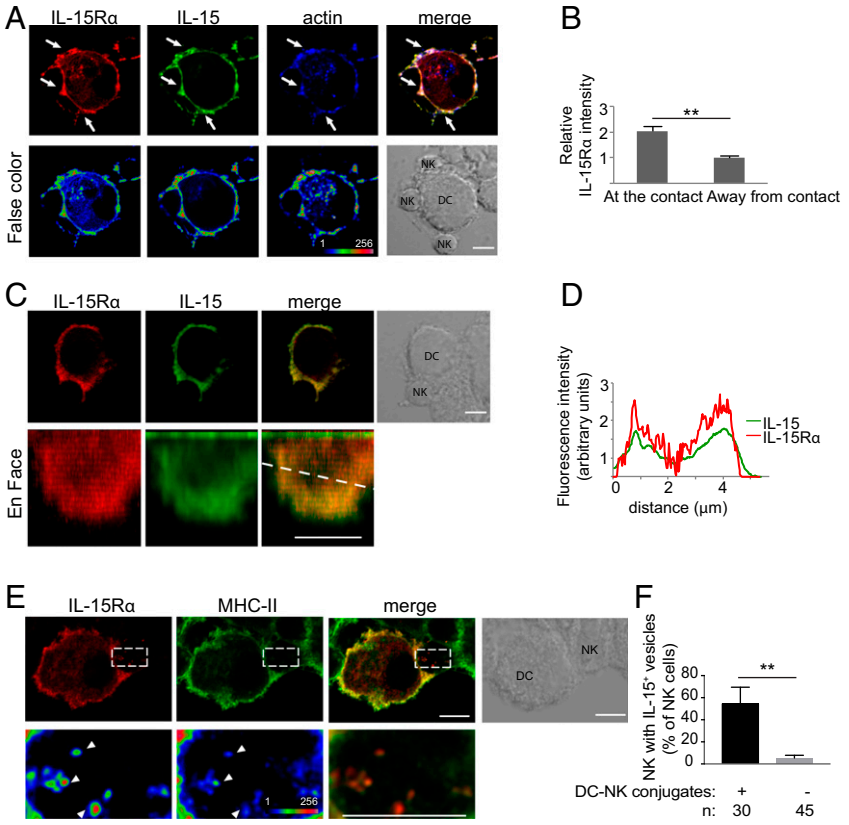

Fig. 2. IL-15Rα is concentrated at DC–NK cell synapses and internalized into NK cells. (*A*) Human monocyte-derived DCs transfected with IL-15Rα-mCherry for 24 h were mixed with autologous primary human NK cells for 30 min. Conjugates were fixed, permeabilized, and stained with anti–IL-15 antibody and phalloidin. (*Lower*) False-color images. Arrows point to sites of IL-15Rα enrichment. (*B*) Enrichment of IL-15Rα at DC–NK cell synapses is represented as the fluorescence intensity at the contact site divided by the fluorescence intensity of a region in which there is no DC–NK cell contact. (*C*) Reconstruction of the synapse area; an en face view is shown. (*D*) Scan of fluorescence intensity of IL-15 and IL-15Rα along the dotted line in *C*. (*E*) DCs transiently transfected with IL-15Rα-mCherry were conjugated with NK cells for 1 h. IL-15Rα was detected in vesicles inside the NK cells. Some of those vesicles also contained MHC-II (arrowheads). (*Lower*) Magnification of the boxed area. (*F*) Frequency of NK cells in conjugates that had IL-15Rα–containing vesicles. *n*, number of cells per condition. The graph represents the mean ± SD of 3 independent experiments. Statistical analysis was performed using a 2-tailed *t* test. (Scale bar: 5 μm.) $^{**}P < 0.01$.

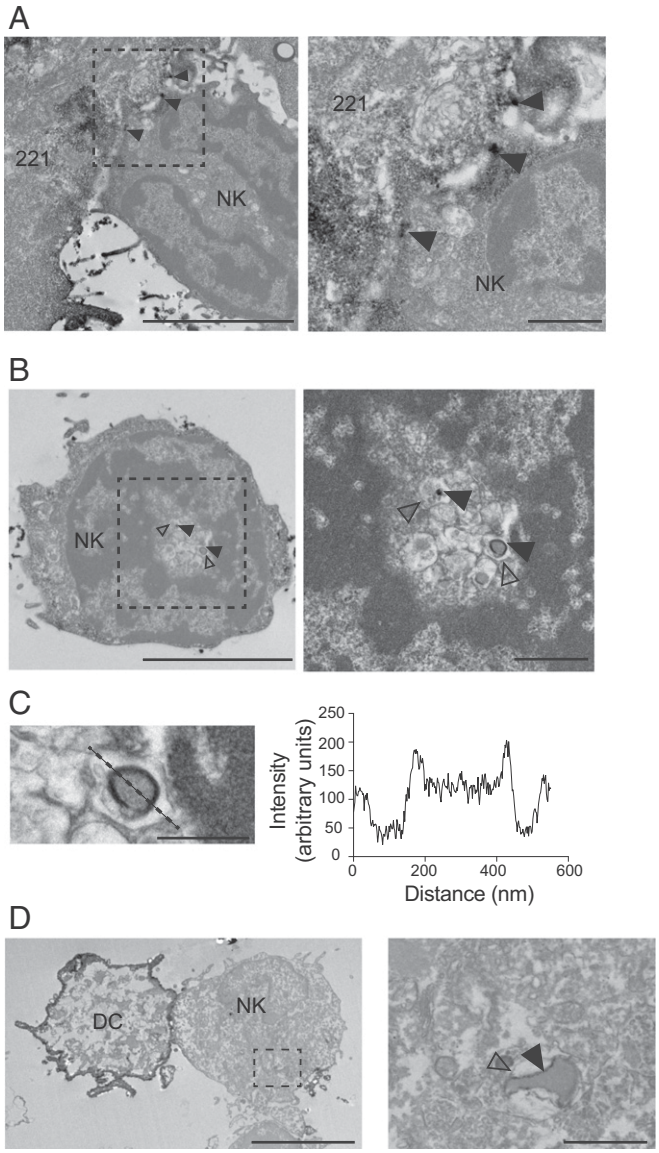

Fig. 3. Detection of IL-15Rα in NK cells on TEM. 221–Venus-IL-15Rα cells were preloaded with IL-15 (5 nM) and conjugated with primary human NK cells for 30 min. Cells were fixed and stained with a polyclonal antibody to GFP and a secondary antibody coupled to peroxidase. IL-15Rα was detected by the presence of an insoluble black precipitate. (*A*) IL-15Rα at the 221–NK cell synapse (arrowheads). (*Right*) Zoom-in view. (Scale bars: 5 μm and 1 μm.) (*B*) IL-15Rα detected inside an NK cell (filled arrowheads). Open arrowheads point to the membrane of the compartment surrounding the IL-15Rα$^+$ vesicle. (*Right*) Zoom-in view. (Scale bars: 5 μm and 1 μm.) (*C*) Detail of the IL-15Rα$^+$ vesicle shown in *B*. The intensity of signal scanned across the vesicle (dotted line) is shown on the right. (Scale bar: 500 nm.) (*D*) Primary DCs expressing Venus-IL-15Rα and preloaded with IL-15 (5 nM) were conjugated with primary autologous human NK cells for 30 min. Cells were fixed and stained as described above. IL-15Rα is detected on a vesicle internalized by the NK cell (filled arrowhead). The open arrowhead indicates the membrane of the vesicle containing the IL-15Rα$^+$ vesicle. (*Right*) Zoom-in view. (Scale bars: 5 μm and 1 μm.)

of the endoplasmic reticulum, we used a modified Cerulean version (oxCerulean3) with mutations that render it resistant to the formation of disulfide bonds while maintaining proper folding, transport to the plasma membrane, and fluorescence (28, 29). 221–Venus–IL-15Rα cells, loaded with IL-15, were mixed with NKL–oxCerulean–IL-2Rβ for 30 min, placed onto coverslips, and fixed. A 3D reconstruction of a conjugate showed Venus-IL-15Rα$^+$ compartments inside the NKL cells, colocalizing with vesicles carrying oxCerulean-IL-2Rβ (arrowheads in Fig. 4*A* and measurements in Fig. 4*C*). By rotating the conjugate 80° along the *y*- axis, an en face view of the contact between the 221 and NKL cells shows colocalization of Venus-IL-15Rα and oxCerulean-IL-2Rβ at the synapse area (arrows in Fig. 4*A* and measurements in Fig. 4*C*). The same conjugation experiment was performed with 221–IL-15Rα-Cherry and NKL–oxCerulean-IL-2Rβ cells. Colocalization of IL-15Rα-Cherry$^+$ puncta inside the NKL cells with vesicles carrying oxCerulean-IL-2Rβ was observed (arrowheads in Fig. 4*B* and measurements in Fig. 4*C*). Colocalization measurements were performed at the synapse and at endocytic vesicles positive for both IL-15Rα and IL-2Rβ (Fig. 4*C*). Mander's coefficients showed colocalization of IL-15Rα with IL-2Rβγ$_c$, suggesting that a fully assembled IL-15Rα–IL-15–IL-2Rβγ$_c$ receptor complex could be signaling while inside the NK cells (Fig. 4*C*). To test this possibility, DCs transfected with IL-15Rα were incubated with NK cells for 30 min. Fixed and permeabilized samples were incubated with an mAb to phosphorylated JAK1. Approximately 56% of vesicles carrying IL-15Rα-Cherry in NK cells had detectable phospho-JAK1 (Fig. 4 *D* and *E*). Note that only *trans*-endocytosed IL-15Rα would retain the mCherry tag in NK cells. These results suggest that *trans*-endocytosed IL-15Rα–IL-15 in NK cells bound IL-2Rβγ$_c$ chains and induced signaling through JAK1 (Fig. 4*D*).

Sensitivity of Stat5 Phosphorylation, but Not S6 Phosphorylation, to Inhibition of IL-15Rα–IL-15 Shedding. IL-15 signals through 2 main pathways, one dependent on Stat5 phosphorylation by JAK1/JAK3 and the other involving an mTOR-Akt–S6 kinase cascade, which results in phosphorylation of the ribosomal protein S6. To test the relative contribution to these 2 pathways of membrane-associated *trans*-endocytic IL-15Rα and of IL-15Rα cleaved from the plasma membrane of *trans*-presenting cells (*SI Appendix*, Fig. S1*B*), we mixed IL-15–loaded 221–IL-15Rα cells with primary NK cells in the presence of GM6001. Phosphorylation of Stat5 and S6 in NK cells was measured by flow cytometry. Phosphorylation of Stat5 was reduced by 60% in the presence of GM6001 (Fig. 5*A*), indicating that shedding of the IL-15Rα–IL-15 complex into a soluble form makes a significant contribution to Stat5 phosphorylation. In contrast, S6 phosphorylation was not affected (Fig. 5*A*), suggesting that something other than shed IL-15Rα–IL-15 is sufficient for S6 phosphorylation. Stat5 and S6 were not phosphorylated in NK cells incubated with 221–IL-15Rα cells that had not been loaded with IL-15 (Fig. 5*A*). There was no significant change in Stat5 and S6 phosphorylation in NK cells incubated with soluble IL-15 or soluble IL-15Rα–IL-15 complex in the presence of GM6001 (Fig. 5*B*), suggesting that the reduction of Stat5 phosphorylation was due to inhibition of IL-15Rα shedding. In accordance with these results, NK cell survival induced by IL-15 *trans*-presentation by 221–IL-15Rα cells was slightly diminished in the presence of GM6001 (Fig. 5*C*), and NK cell proliferation remained unaltered in the presence of GM6001 (Fig. 5*D* and *SI Appendix*, Fig. S1*D*). These data support the hypothesis that in our IL-15 *trans*-presentation system, soluble IL-15Rα–IL-15 complex contributes mainly to the Stat5 pathway and suggest that IL-15 *trans*-presented by membrane-bound IL-15Rα–IL-15 may be required for efficient phosphorylation of S6.

Phosphorylation of Stat5 and of S6 in primary NK cells was measured after stimulation for 15 min with a broad range of concentrations of soluble IL-15 and soluble IL-15Rα–IL-15 complex. Stat5 phosphorylation was biphasic (Fig. 5*C*). In the first phase, half-maximal Stat5 phosphorylation occurred at 10 pM IL-15Rα–IL-15 and reached a plateau at 100 pM. In contrast, S6 phosphorylation was barely detectable at 10 pM and reached the half-maximum at 200 pM IL-15Rα–IL-15 (Fig. 5*C*). The second phase of Stat5 phosphorylation showed properties similar to those of S6 phosphorylation. Under saturation conditions, soluble

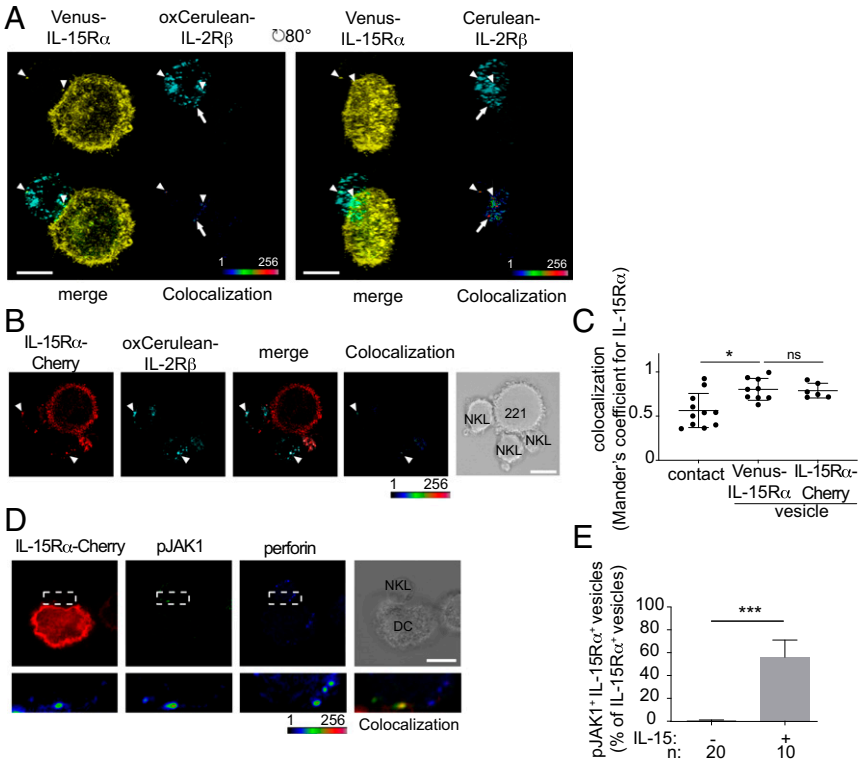

Fig. 4. IL-15Rα transferred into NK cells colocalizes with IL-2Rβ and is signaling-competent. (*A*) 221–Venus-IL-15Rα cells preloaded with 5 nM IL-15 were conjugated with NKL–oxCerulean-IL-2Rβ for 30 min. A 3D reconstruction of a conjugate is shown from an upper view or rotated 80°. Colocalization is shown as a false-color intensity scale. IL-15Rα colocalizes with IL-2Rβ in vesicles inside NK cells (arrowheads) and at the contact area (arrows). (*B*) 221–IL-15Rα-Cherry cells preloaded with 5 nM IL-15 were conjugated with NKL–oxCerulean-IL-2Rβ for 30 min. The image shows a conjugate with 3 NKL cells. Colocalization of IL-15Rα-Cherry and oxCerulean-IL-2Rβ can be appreciated in vesicles (arrowheads) and is represented as a false-color intensity scale image. (*C*) Colocalization of IL-15Rα and IL-2Rβ at the synapse or inside NK cells was measured using Fiji software and expressed as Mander's coefficients. $*P < 0.05$. (*D*) Human monocyte-derived DCs were transiently transfected with IL-15Rα-mCherry for 24 h and then mixed with NKL cells for 30 min. Conjugates were fixed, permeabilized, and stained with an antibody to phosphorylated JAK1 (pJAK1) and an anti-perforin antibody to distinguish NK cells from IL-15Rα-mCherry–negative DCs. (*Lower*) Magnification of the synapse area indicated by the white dotted box. (*E*) Quantitation of IL-15Rα and pJAK1 colocalization inside NK cells from different experiments. *n* represents the number of cells per condition. Statistical analysis was performed using a 2-tailed *t* test. $***P < 0.001$.

IL-15 and soluble IL-15Rα–IL-15 complex stimulated phosphorylation of Stat5 with similar magnitude and kinetics. Likewise, S6 phosphorylation was equally strong during stimulation with soluble IL-15 and soluble IL-15Rα–IL-15 complex, with perhaps greater phosphorylation early after addition of the complex (*SI Appendix*, Fig. S1*E*). These results suggest that NK cell survival would require much less IL-15 than NK cell proliferation. Survival of primary NK cells was indeed improved at 0.25 pM IL-15Rα–IL-15, with further improvement at 250 pM (Fig. 5*D*). In contrast, NK cell proliferation was not detected at 0.25 pM but occurred at 250 pM and was further improved at 250 nM (Fig. 5*E*). We conclude that soluble IL-15 and IL-15Rα–IL-15 complex were weaker stimulators of S6 phosphorylation and NK cell proliferation compared with stimulation of Stat5 phosphorylation and NK cell survival. Considering the high efficiency of Stat5 phosphorylation in response to soluble IL-15Rα–IL-15 compared with S6 phosphorylation, it is remarkable that S6 phosphorylation was not sensitive to inhibition of shedding by GM6001 (Fig. 5*A*).

Stimulation of Stat5 and S6 Phosphorylation by IL-15Rα–IL-15 Complex Immobilized on Large Beads. To mimic IL-15 *trans*-presentation at the plasma membrane, occurring in the absence of shedding and of *trans*-endocytosis, we generated 6-μm latex beads carrying a covalently bound, recombinant IL-15Rα–IL-15 complex that lacked the MMP-sensitive membrane-proximal domain (24, 27). These beads formed conjugates with NK cells, as shown by flow cytometry and confocal microscopy (*SI Appendix*, Fig. S2 *A* and *B*). These beads were rarely internalized by the NK cells (*SI Appendix*, Fig. S2*B*). For a reference, we first performed a time course of stimulation with soluble IL-15. At a high concentration (100 nM), IL-15 induced rapid phosphorylation of Stat5, which peaked at 30 min, and a slower and gradual increase in S6 phosphorylation over 3 h (Fig. 6*A* and *SI Appendix*, Fig. S2). Beads were coated with different amounts of IL-15Rα–IL-15, resulting in beads presenting with low, medium, and high ligand densities (Fig. 6*B*). Stimulation of Stat5 and S6 phosphorylation in primary NK cells by beads was measured by flow cytometry and is shown relative to maximal stimulation obtained with soluble IL-15 (Fig. 6 *C*–*E*). Beads with a low density of IL-15Rα–IL-15 stimulated Stat5 phosphorylation, which reached 35% of control at 60 min, but did not induce S6 phosphorylation (Fig. 6*C*). Stat5 phosphorylation equal to the maximal reference value was reached by stimulation with medium-density beads, whereas S6 phosphorylation reached 35% of control (Fig. 6*D* and *SI Appendix*, Fig. S2). S6 phosphorylation reached 80% of control after stimulation with high-density beads (Fig. 6*E*). These results show that engagement of IL-2Rβ–γ_c at the plasma membrane of NK cells by *trans*-presented IL-15Rα–IL-15 can activate both pathways. However, S6 phosphorylation was much more dependent on ligand density than Stat5 phosphorylation. Consistent with these results, substantial NK cell proliferation was activated only by beads with high IL-15Rα–IL-15 density (Fig. 6*F*). In contrast, survival of freshly isolated NK cells was promoted equally well by medium-density and high-density beads (Fig. 6*G*).

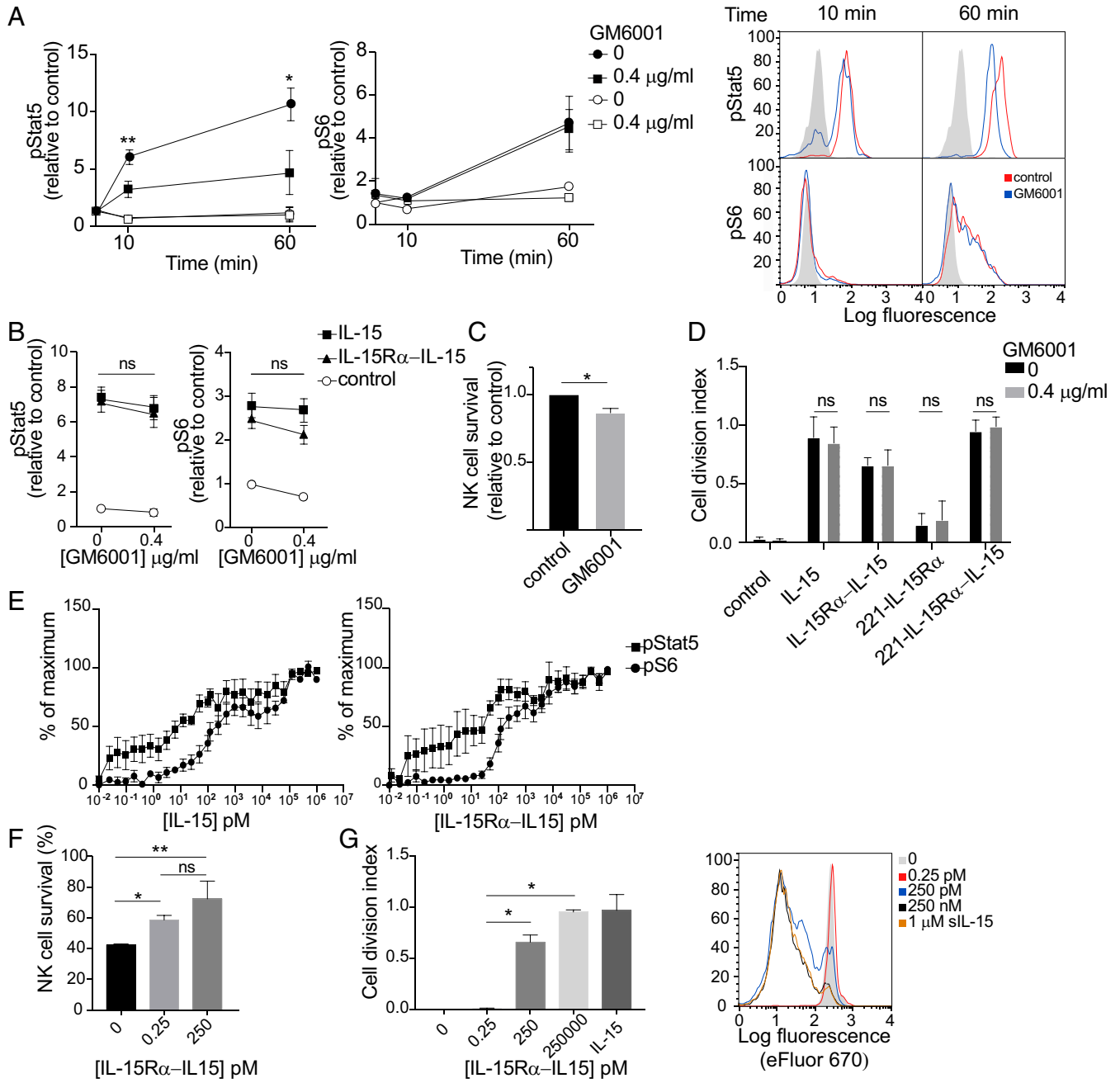

Fig. 5. Soluble IL-15Rα–IL-15 complex generated by shedding during *trans*-presentation contributes to phosphorylation of Stat5, but not of S6. (*A*) 221–IL-15Rα cells preloaded (filled symbols) or not (open symbols) with IL-15 were preincubated with 0.4 μg/mL GM6001 for 10 min and then conjugated with primary human NK cells for 10 min and 60 min in the same concentration of GM6001. Cells were fixed at the indicated time points, permeabilized, and stained with antibodies to phosphorylated Stat5 (pStat5) and phosphorylated S6 (pS6) by flow cytometry. Graphs show mean fluorescence values relative to untreated NK cells of 3 independent experiments. Bars represent the SD of the mean. Representative flow histograms are shown on the right. Shaded histograms represent the staining at time 0. (*B*) Primary human NK cells were incubated with 0.4 μg/mL GM6001 and 100 nM soluble IL-15 or soluble IL-15Rα–IL-15 complex for 1 h. Cells were fixed, permeabilized, and stained with antibodies to pStat5 and pS6 and then analyzed by flow cytometry. Graphs show mean fluorescence values relative to untreated NK cells of 3 independent experiments. Bars represent the SD of the mean. ns, not significant. (*C*) Primary human NK cells were mixed with 221–IL-15Rα cells preloaded with IL-15 in the presence or absence of GM6001. The fraction of NK cells that remained alive after 5 d was counted and expressed relative to control GM6001-untreated cells. (*D*) Primary human NK cells were loaded with eFluor 670 and stimulated with soluble IL-15, soluble IL-15Rα–IL-15 complex, or 221–IL-15Rα cells, loaded or not with IL-15, in the presence of GM6001 for 5 d. Cell division of $CD56^+$ cells was !evaluated by flow cytometry, and the cell division index (i.e., average number of cell divisions undergone by a cell in the original population) was calculated. The histograms show the mean ± SD of 3 independent experiments. A representative experiment is shown on the right. Black and shaded histograms represent eFluor signals for unstimulated NK cells in the presence or absence of GM6001. (*E*) Primary human NK cells were stimulated with soluble IL-15 (*Left*) or soluble IL-15Rα–IL-15 complex (*Right*) at the indicated concentrations for 1 h. Cells were fixed, permeabilized, stained with antibodies to pStat5 and pS6, and analyzed by flow cytometry. Graphs represent the mean and SEM of 6 different donors. Values are relative to a maximum, defined as a pStat5 or pS6 signal obtained after incubation with 1 μM of either soluble IL-15 or soluble IL-15Rα–IL-15 complex for 60 min. (*F*) Primary human NK cells were stimulated with soluble IL-15Rα–IL-15 complex at the indicated concentrations for 5 d. The fraction of NK cells that remained alive was counted after 5 d. (*G*) Primary human NK cells were loaded with eFluor 670 and stimulated with soluble IL-15Rα–IL-15 complex at the indicated concentrations for 5 d. Cell division of $CD56^+$ cells was evaluated by flow cytometry, and the cell division index was calculated. 1 μM soluble IL-15 (sIL-15) added to the NK cells served as a control of maximum NK proliferation. A representative experiment is shown at the right. Statistical analysis was performed using a 2-tailed *t* test. $^*P < 0.05$; $^{**}P < 0.01$.

Regulation of IL-15Rα–IL-15 *Trans*-Endocytosis and S6 Phosphorylation by the Small GTPase TC21. TC21 is a small GTPase encoded by the *RRAS2* gene, which is ubiquitously expressed in leukocytes and plays a role in *trans*-endocytosis of MHC from antigen-presenting cells to T cells (26). To test its contribution to IL-15Rα–IL-15 *trans*-endocytosis into NK cells, TC21 was silenced by siRNA in primary NK cells, which resulted in a 50% reduction in the amount of TC21 protein (Fig. 7 *A* and *B*). In TC21-depleted NK cells, uptake of IL-15Rα-Cherry from IL-15–preloaded 221–IL-15Rα-Cherry cells was reduced to a similar extent (Fig. 7*C*), consistent with a similar role of TC21 for *trans*-endocytosis into NK cells. Furthermore, phosphorylation of S6, but not of Stat5, was reduced in TC21-depleted NK cells after incubation with 221–IL-15Rα cells that had been loaded with IL-15 (Fig. 7*D* and *SI Appendix*, Fig. S3*A*). TC21 depletion did not impair S6 phosphorylation directly, as it had no effect on Stat5 and S6 phosphorylation stimulated by a high dose of soluble IL-15 (Fig. 7 *E* and *F*). Adhesion of NK cells with 221–IL-15Rα *trans*-presenting cells was not significantly inhibited by TC21 depletion, as shown by a conjugation assay (*SI Appendix*, Fig. S3*B*). These data support the view that TC21 depletion in NK cells inhibits the phosphorylation of S6 induced specifically by *trans*-endocytosis of IL-15Rα from *trans*-presenting cells.

To further test the contribution of TC21-dependent IL-15Rα–IL-15 *trans*-endocytosis to S6 phosphorylation, a dominant-negative (DN) TC21 mutant (Ser28Asn) was expressed in NKL cells (*SI Appendix*, Fig. S3*C*). In 2 independent clones of NKL–TC21DN-GFP cells, phosphorylation of S6 induced by conjugation with IL-15–loaded 221–IL-15Rα cells was reduced compared with that in NKL cells expressing wild-type TC21-GFP (Fig. 7 *G* and *H*). In contrast, phosphorylation of Stat5 was not reduced in NKL–TC21DN-GFP cells (Fig. 7*H*). Therefore, something other than a TC21-dependent step is sufficient for optimal stimulation of Stat5 phosphorylation. Dominant-negative TC21 did not inhibit signal transduction for S6 phosphorylation, as it had no effect on S6 phosphorylation induced by soluble IL-15 (Fig. 7*I*). Adhesion of NKL cells with 221–IL-15Rα *trans*-presenting cells was not significantly inhibited by TC21 depletion, as shown in a conjugation assay (*SI Appendix*, Fig. S3*D*). These results confirm that a TC21-dependent step is required for proper S6 phosphorylation and

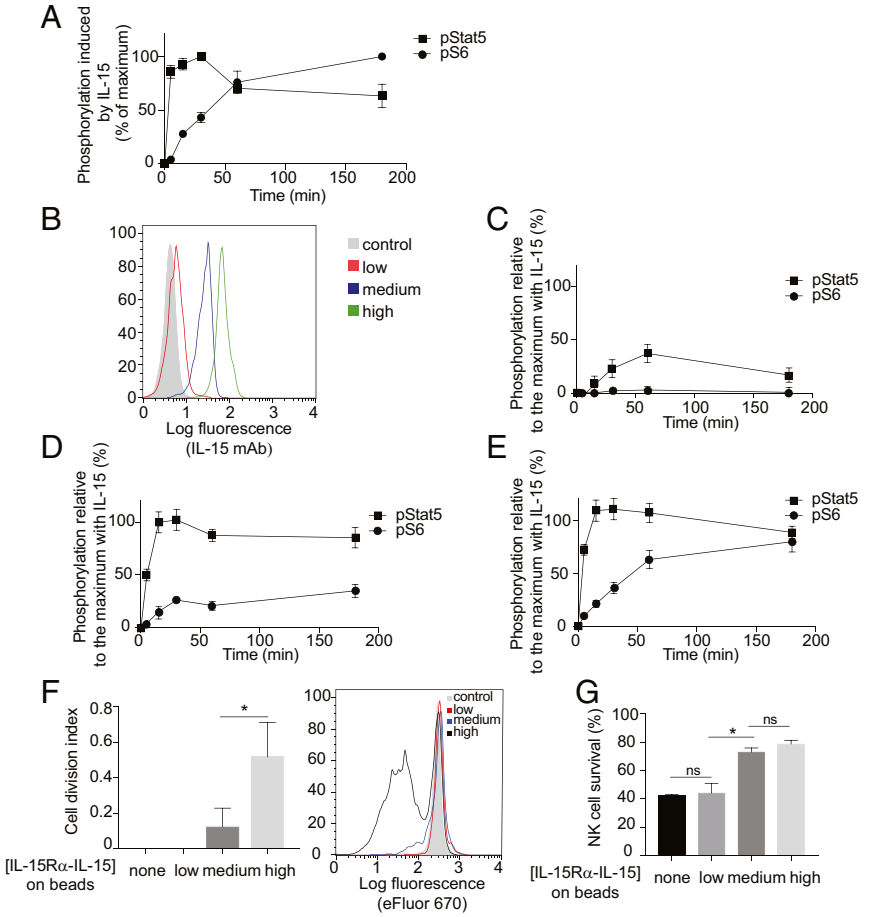

Fig. 6. Stimulation of Stat5 and S6 phosphorylation by IL-15Rα–IL-15 complex immobilized on large beads. (*A*) Time course of Stat5 and S6 phosphorylation in primary NK cells during incubation with 100 nM soluble IL-15. Data are shown as relative to the highest data point (30 min for Stat5 and 3 h for S6). (*B*) Purified recombinant IL-15Rα–IL-15 complex was covalently coupled to beads at different concentrations, resulting in beads carrying different densities (low, medium, and high) of IL-15Rα–IL-15. Beads were stained with a monoclonal antibody to IL-15 and a secondary antibody coupled to allophycocyanin. The shaded histogram represents staining in the absence of primary antibody. (*C*–*E*) Primary NK cells were incubated with beads covalently coupled to IL-15Rα–IL-15, at a 1:1 NK:bead ratio for the indicated times. Graphs show the mean fluorescence values of 3 independent experiments relative to the maximum phosphorylation of Stat5 or S6 obtained after the addition of 100 nM soluble IL-15. Beads had been coated with a low (*C*), medium (*D*), or high (*E*) density of IL-15Rα–IL-15 complex. (*F*) The cell division index after 5 d was calculated. A representative experiment is shown at the right. Control cells represent NK cells incubated with beads in the absence of coupled IL-15Rα–IL-15. (*G*) Primary human NK cells loaded with 5 μM eFluor 670 were stimulated with IL-15Rα–IL-15 coupled to beads at the indicated densities. After 5 d, $CD56^+$ cells were assessed by flow cytometry. Results are expressed as the fraction of NK cells that remained alive. Statistical analysis was performed using a 2-tailed *t* test. ns, not significant. $*P < 0.05$; $**P < 0.01$.

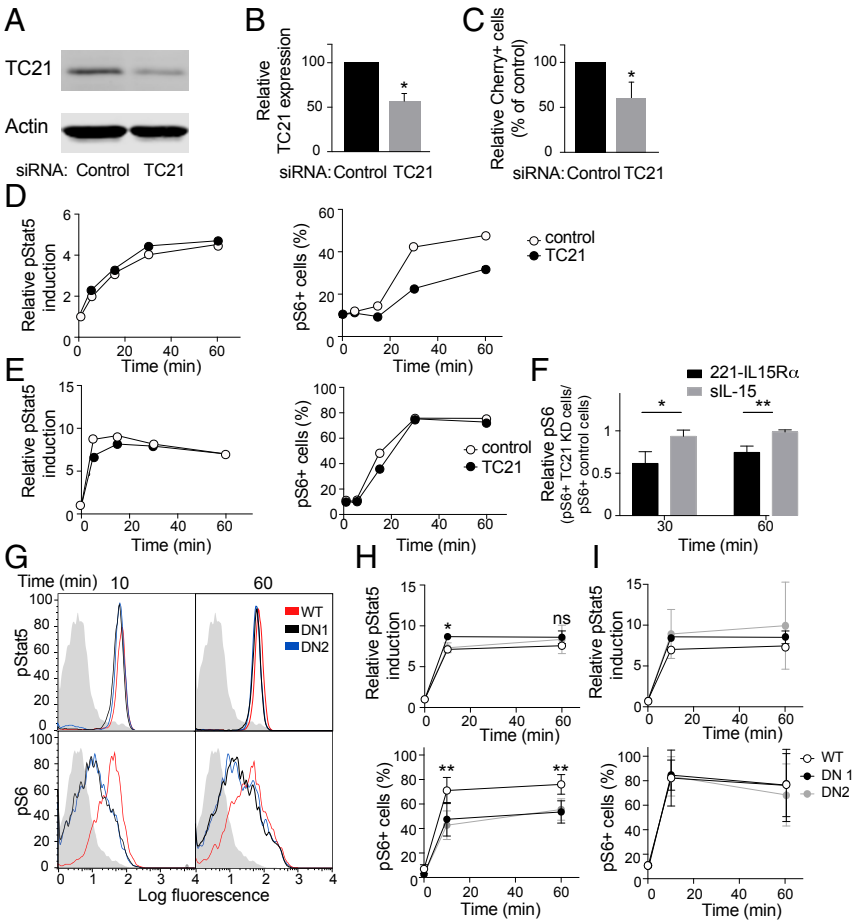

Fig. 7. Regulation of IL-15Rα–IL-15 *trans*-endocytosis and S6 phosphorylation by the small GTPase TC21. (*A*) Immunoblots of TC21 and actin from lysates of IL-2–activated human NK cells transfected with control siRNA or a pool of siRNA to TC21. (*B*) TC21 silencing determined by immunoblotting in 3 different experiments, relative to the siRNA control. The quantitation was relative to actin. The graph represents mean ± SD. (*C*) TC21-silenced and control primary IL-2–activated NK cells were conjugated for 60 min with 221–IL-15Rα-Cherry cells that had been preloaded with IL-15. The percentage of Cherry$^+$ TC21-silenced NK cells was determined by flow cytometry, gating on CD56$^+$ cells, and is shown as relative to the percentage of Cherry$^+$ siRNA control-transfected NK cells. The graph shows the mean and SEM of 3 independent experiments. (*D*) TC21-silenced and siRNA control-transfected NK cells were incubated for the indicated times with 221–IL-15Rα cells that had been preloaded with IL-15. Phosphorylation of Stat5, as relative to time 0, and S6, as a percentage of positive cells (mean fluorescence intensity >10^1), was measured by flow cytometry. A representative experiment is shown. (*E*) TC21-silenced and siRNA control-transfected NK cells were incubated with 100 nM soluble IL-15 for the indicated times and analyzed as in *D*. A representative experiment is shown. (*F*) pS6 relative phosphorylation in siRNA control-transfected and TC21-silenced NK cells at 30 and 60 min in cells conjugated with 221–IL-15Rα or stimulated with soluble IL-15. The graph shows the mean and SD of 3 independent experiments. (*G*) NKL cells stably expressing either TC21 wild-type (WT) or DN (clones DN1 and DN2) were incubated for the indicated times with 221–IL-15Rα cells that had been preloaded with IL-15. Phosphorylation of Stat5 and S6 was measured by flow cytometry. A representative experiment is shown. Shaded histograms represent the staining of pStat5 or pS6 at 0 min. (*H*) Quantitation of 3 independent experiments. Phosphorylation of Stat5, as relative to time 0, and S6, as a percentage of positive cells, is represented. Graphs show mean ± SD values. (*I*) Graphs showing phosphorylation of Stat5 and S6 in response to soluble IL-15 in NKL cells expressing TC21 WT or DN constructs (mean ± SD). Statistical analysis was performed using a 2-tailed *t* test (*B*, *C*, and *F*) or 2-way analysis of variance (*H* and *I*). *$P < 0.05$; **$P < 0.01$.

proliferation. This finding, along with the clear evidence of *trans*-endocytosis of IL-15Rα–IL-15 into NK cells, supports the conclusion that *trans*-endocytosis favors S6 phosphorylation.

Discussion

IL-15 is essential for NK cell survival, development, proliferation, and function (1, 15). In contrast to the related cytokine IL-2, IL-15 is usually presented in *trans* by cells expressing an IL-15Rα–IL-15 complex at their surface, such as DCs. The goal of our study was to test the functional outcome of IL-15 *trans*-presentation to NK cells through different pathways, with a focus on signals for survival and proliferation.

Three modes of *trans*-presentation can be considered (*SI Appendix*, Fig. S1*B*). First, the IL-15Rα–IL-15 complex on *trans*-presenting cells binds to the β-γ_c subunits of IL-2R at the plasma membrane of NK cells, and signaling occurs there. This interaction would occur alongside the many receptor–ligand interactions that take place at NK cell immunologic synapses. In a second scenario, the IL-15Rα–IL-15 complex is transferred from *trans*-presenting cells to NK cells, which could occur in 2 ways. Shedding of a soluble form of IL-15Rα–IL-15 from *trans*-presenting cells through the activity of cell surface metalloproteases produces a ligand for IL-2Rβ-γ_c. The soluble IL-15Rα–IL-15 complex transferred to NK cells could then be endocytosed with IL-2Rβ-γ_c. Finally, *trans*-endocytosis of a vesicle snatched from the plasma membrane of *trans*-presenting cells into NK cells would result in a double-membrane intracellular compartment where *trans*-presentation persists (*SI Appendix*, Fig. S1*B*). This would be a different type of endosome, with a different topology, into which the quaternary IL-15 complex is *trans*-endocytosed along with a fragment of the

DC plasma membrane. Signaling by the quaternary IL-15 complex could differ from signaling by endocytosed soluble IL-15Rα–IL-15 complex. It could be more stable and could couple to different signaling platforms present on these different kinds of endosomes. It is worth noting that this topology would be identical to that of IL-15Rα–IL-15^{+} exosomes internalized by NK cells. NK cell activation and proliferation induced by DC-derived exosomes has been reported (30). NK cell activation through *trans*-endocytosis by either of these pathways would be independent of cell surface metalloproteases and could avoid interference by other receptor–ligand interactions at immunologic synapses.

Using IL-15Rα tagged on the cytosolic tail with a fluorescent protein to monitor transfer to NK cells of an intact, membrane-associated IL-15Rα expressed in DCs, we detected it in intracellular compartments of primary, freshly isolated NK cells. TEM images revealed characteristic double-membrane vesicles, as expected of a *trans*-endocytosis mechanism for transfer. *Trans*-endocytosed IL-15Rα–IL-15 colocalized with IL-2Rβ in intracellular compartments in NK cells. Furthermore, colocalization of IL-15Rα-Cherry in intracellular vesicles with phosphorylated JAK1 indicated that this was a signaling-competent interaction.

Phosphorylation of Stat5 by JAK3 initiates a signaling pathway that is required for NK cell survival (15, 31). The signaling pathway for NK cell proliferation induced by IL-2Rβ-γ_c includes a PI-3K–Akt–mTOR–S6 kinase axis (19, 32). Multiple factors appear to play a role in how IL-15Rα–IL-15 signaling yields distinct functional outcomes. Strength of signal is clearly one factor for stimulation with soluble IL-15 or IL-15 complex. Very low concentrations of IL-15Rα–IL-15 complex are sufficient to activate the JAK/Stat pathway and yield pStat5, compared with the concentrations needed to stimulate pS6. Upon stimulation by IL-15Rα–IL-15 coupled to beads, in the absence of soluble and of *trans*-endocytosed IL-15, Stat5 phosphorylation is also more efficient, as it requires a lower IL-15Rα–IL-15 density for optimal stimulation than that required for optimal S6 phosphorylation. The data presented here add another dimension, in that the cellular compartment in which receptor–ligand interactions occur can have an effect on functional outcome. In particular, Stat5 phosphorylation, but not S6 phosphorylation, was sensitive to inhibition of IL-15Rα–IL-15 shedding. Even though shed IL-15Rα–IL-15 does not seem to be required for optimal S6 phosphorylation, it makes a significant contribution to Stat5 phosphorylation. Conversely, optimal IL-15Rα–IL-15 *trans*-endocytosis and S6 phosphorylation were dependent on the small GTPase TC21, while Stat5 phosphorylation was not, suggesting that the encounter of an intact, membrane-associated IL-15Rα–IL-15 with IL-2Rβ-γ_c in an NK endosome that has engulfed a piece of DC membrane is a better location to signal for proliferation. In the case of T cells, the *trans*-endosomes generated after contact with antigen-presenting cells have been shown to promote a more sustained TCR signal (33).

Shedding of soluble IL-15Rα–IL-15 from transfected HEK-293 cells also has been reported to stimulate Stat5 phosphorylation in a T cell line (25). The benefit of NK cell stimulation through shedding of IL-15Rα–IL-15, which contributes to Stat5 phosphorylation, may be a reduced dependence on sustained cell–cell contacts supplanted by sustained signaling in endosomes by soluble IL-15Rα–IL-15 bound to IL-2Rβ-γ_c. As soluble IL-15 or soluble IL-15Rα–IL-15 complex is at very low or undetectable levels in human tissues under normal conditions (23, 34), NK cell survival is dependent on contact with *trans*-presenting cells (35) where direct transfer of IL-15Rα–IL-15 shed at the immunologic synapse can occur efficiently.

The small Ras-related GTPase TC21 in T cells is required for *trans*-endocytosis of the MHC on antigen-presenting cells into T cells (26). A recent quantitative proteomics analysis of human leukocyte subsets revealed a high abundance of TC21 in NK cells (36). Silencing TC21 in primary NK cells inhibited *trans*-endocytosis of intact, membrane-associated IL-15Rα–IL-15 from *trans*-presenting cells without impairing DC–NK cell conjugate formation. TC21 silencing reduced the phosphorylation of S6 but had no effect on Stat5 phosphorylation. These results were confirmed independently by generating NK cell lines expressing a dominant-negative mutant of TC21, reinforcing the hypothesis that the *trans*-endocytosis pathway supports S6 phosphorylation and NK cell proliferation. In this regard, it is worth noting that *trans*-endocytosis endows IL-15 with properties not available to IL-2.

How is *trans*-endocytosis qualitatively and functionally different from endocytosis? Endocytosis brings molecules tethered to the plasma membrane into endosomal compartments. Internalization of receptors at the plasma membrane on binding of soluble ligand, such as IL-2 receptor in the presence of IL-2 (37–39), is very common. Signaling from endosomes by receptors that have been internalized is now a well-accepted mode of signaling with more sustained responses, unique effectors, and distinct outcomes compared with those induced by signaling at the cell surface (40). *Trans*-endocytosis has an added layer of complexity, involving the exchange of membrane domains between cells (*SI Appendix*, Fig. S1*B*). The persistence of IL-15 *trans*-presentation in endosomes as an interaction between 2 receptors, each anchored on a different membrane, may be a benefit of *trans*-endocytosis. Once *trans*-endocytosed, IL-15Rα–IL-15 bound to IL-2Rβ-γ_c may be sheltered from control by other receptor–ligand interactions occurring at the DC–NK immunologic synapse, such as inhibition by killer-cell Ig-like receptors binding to HLA-C on *trans*-presenting cells (19). As we show here, *trans*-endocytosis of IL-15Rα–IL-15 appears to have functional consequences distinct from stimulation by soluble IL-15Rα–IL-15. While there was no reduction in S6 phosphorylation after blocking of MMP-dependent release of IL-15Rα–IL-15 as a soluble complex, *trans*-endocytosis promoted phosphorylation of ribosomal protein S6, which is required for proliferation.

Our results provide insight into the regulation of IL-15–dependent responses and show that *trans*-presentation of IL-15 occurs through different pathways with distinct functional outcomes. This opens up the potential for new approaches to regulating NK cells, which could have implications for the stimulation of NK cells used in cancer immunotherapy.

Materials and Methods

Cells. Human NK cells were isolated from peripheral blood mononuclear cells (PBMCs) by negative selection using magnetic beads (Miltenyi Biotech). Peripheral blood samples from healthy US adults were obtained from the NIH Department of Transfusion Medicine under an NIH Institutional Review Board-approved protocol (99-CC-0168) with informed consent. NK cell purity was assessed by flow cytometry; cells were ≥98% CD3^{-}CD56^{+}NKp46^{+}. Human DCs were differentiated from monocytes isolated from PBMCs by negative selection using magnetic beads (Miltenyi Biotech). Cell purity was assessed by flow cytometry; cells were ≥98% CD3^{-}CD11c^{+}CD56^{-}. To differentiate them into DCs, the isolated monocytes were cultured for 6 d in Iscove's Modified Dulbecco's Medium with 10% human serum containing 100 ng/mL IL-4 and 50 ng/mL granulocyte macrophage colony-stimulating factor (GM-CSF). On day 6, 1 μg/mL lipopolysaccharide was added. On day 7, the differentiated DCs were tested for positive expression of CD11c, CD83, and IL-15Rα and up-regulation of MHC-I. The human NK cell line NKL was cultured in Roswell Park Memorial Institute (RPMI) medium supplemented with 10% FBS and 100 U/mL rIL-2. NKL–oxCerulean-IL-2Rβ, NKL–TC21WT-GFP, and NKL–TC21DN-GFP cells were generated by lentiviral transduction and selected with 0.3 μg/mL puromycin. Human B lymphoblastoid 721.221 cells (41) expressing IL-15Rα (221–IL-15Rα) and IL-15Rα-Cherry (221–IL-15Rα-Cherry) have been described previously (19). The 721.221 cells expressing Venus-IL-15Rα (221–Venus-IL-15Rα) were transfected by electroporation and selected with 3.4 μg/mL blasticidin. Transfected 721.221 cells were maintained in RPMI medium supplemented with 10% FBS and L-glutamine.

The study was performed in accordance with the Declaration of Helsinki's ethical principles of medical research. All patients provided signed informed consent for participation in clinical studies. The clinical studies were approved by the Intramural Review Board of the National Cancer Institute, NIH.

Antibodies and Reagents. The following antibodies were used: polyclonal anti-GFP antibody (Abcam), anti–phospho-Ser235Ser236-S6 (2F9) coupled to Alexa Fluor 488 (Cell Signaling), anti–phospho-Tyr694-Stat5 coupled to Alexa Fluor 647 and anti-CD56 coupled to phycoerythrin (PE; BD Biosciences), anti–phospho-Tyr1022-JAK1 (Santa Cruz Biotechnology), anti-human IL-15Rα mAb (10), anti-human IL-15 (R&D Systems), and anti-perforin (Thermo Fisher Scientific). Secondary anti-rabbit IgG and anti-mouse IgG antibodies coupled to Alexa Fluor 488 were obtained from Molecular Probes; secondary anti-mouse IgG antibody coupled to PE and secondary Fab2 anti-rabbit IgG coupled to HRP were obtained from The Jackson Laboratory, and anti-TC21 Ab was a kind gift from B. Alarcon, Centro de Biología Molecular Severo Ochoa, Madrid, Spain, and has been described previously (42).

Human IL-2, IL-4, IL-15, and GM-CSF cytokines were obtained from Peprotech; LPS from bacteria was obtained from Sigma-Aldrich; and MMP inhibitor GM6001 was obtained from EMD Millipore. The soluble IL-15Rα–IL-15 complex was prepared as described previously (27).

IL-15 Loading for *Trans*-Presentation by IL-15Rα–Transfected Cells. For *trans*-presentation experiments, 721.221 cells expressing IL-15Rα were resuspended in RPMI medium and incubated for 20 min at 37 °C in 5% CO_2 with soluble IL-15 at a final concentration of 100 ng/mL. The cells were then washed 3 times in complete RPMI medium.

Intracellular Flow Cytometry and Immunofluorescence Analysis. Both methods have been described previously (19), and complete details are provided in *SI Appendix*.

Coupling of IL-15Rα–IL-15 to Latex Beads. Here 6 μM 488 fluorescent latex beads (microspheres; Polysciences) were activated using a C-terminal carboxy kit (Polysciences) following the manufacturer's protocol. The beads were then incubated with different concentrations of IL-15Rα–IL-15 complex for 3 h at room temperature. Coupling to the beads was verified by flow cytometry.

Statistical Analysis. Differences between datasets were analyzed with a 2-tailed *t* test (unpaired or paired) or ANOVA (paired) using GraphPad Prism or Microsoft Excel. The number of repeats is specified for each experiment. For imaging experiments, *n* refers to the number of cells analyzed. Error bars denote SD or SEM.

Data Availability. All data discussed in the paper are included in the manuscript and *SI Appendix*.

ACKNOWLEDGMENTS. We thank A. Ring and M. Rizzo for advice; and B. Alarcon for the TC21-GFP plasmids (wild-type and dominant negative) and the antibody against TC21. This work was supported by the NIH Intramural Research Programs at the National Institute of Allergy and Infectious Diseases (E.O.L.), and the National Cancer Institute, Center for Cancer Research (T.A.W.).

1. M. A. Caligiuri, Human natural killer cells. *Blood* **112**, 461–469 (2008).
2. T. A. Fehniger, M. A. Caligiuri, Interleukin 15: Biology and relevance to human disease. *Blood* **97**, 14–32 (2001).
3. Y. Rochman, R. Spolski, W. J. Leonard, New insights into the regulation of T cells by gamma(c) family cytokines. *Nat. Rev. Immunol.* **9**, 480–490 (2009).
4. J. P. DiSanto, W. Müller, D. Guy-Grand, A. Fischer, K. Rajewsky, Lymphoid development in mice with a targeted deletion of the interleukin-2 receptor gamma chain. *Proc. Natl. Acad. Sci. U.S.A.* **92**, 377–381 (1995).
5. T. Kawamura, R. Koka, A. Ma, V. Kumar, Differential roles for IL-15R alpha-chain in NK cell development and Ly-49 induction. *J. Immunol.* **171**, 5085–5090 (2003).
6. M. K. Kennedy *et al.*, Reversible defects in natural killer and memory CD8 T cell lineages in interleukin-15-deficient mice. *J. Exp. Med.* **191**, 771–780 (2000).
7. J. P. Lodolce *et al.*, IL-15 receptor maintains lymphoid homeostasis by supporting lymphocyte homing and proliferation. *Immunity* **9**, 669–676 (1998).
8. H. Suzuki, G. S. Duncan, H. Takimoto, T. W. Mak, Abnormal development of intestinal intraepithelial lymphocytes and peripheral natural killer cells in mice lacking the IL-2 receptor beta chain. *J. Exp. Med.* **185**, 499–505 (1997).
9. C. A. Vosshenrich *et al.*, Roles for common cytokine receptor gamma-chain-dependent cytokines in the generation, differentiation, and maturation of NK cell precursors and peripheral NK cells in vivo. *J. Immunol.* **174**, 1213–1221 (2005).
10. S. Dubois, J. Mariner, T. A. Waldmann, Y. Tagaya, IL-15Ralpha recycles and presents IL-15 in trans to neighboring cells. *Immunity* **17**, 537–547 (2002).
11. H. Kobayashi *et al.*, Role of trans-cellular IL-15 presentation in the activation of NK cell-mediated killing, which leads to enhanced tumor immunosurveillance. *Blood* **105**, 721–727 (2005).
12. E. Mortier, T. Woo, R. Advincula, S. Gozalo, A. Ma, IL-15Ralpha chaperones IL-15 to stable dendritic cell membrane complexes that activate NK cells via trans presentation. *J. Exp. Med.* **205**, 1213–1225 (2008).
13. R. Koka *et al.*, Interleukin (IL)-15R[alpha]-deficient natural killer cells survive in normal but not IL-15R[alpha]-deficient mice. *J. Exp. Med.* **197**, 977–984 (2003).
14. S. W. Stonier, K. S. Schluns, Trans-presentation: A novel mechanism regulating IL-15 delivery and responses. *Immunol. Lett.* **127**, 85–92 (2010).
15. E. Eckelhart *et al.*, A novel Ncr1-Cre mouse reveals the essential role of STAT5 for NK-cell survival and development. *Blood* **117**, 1565–1573 (2011).
16. A. Ma, R. Koka, P. Burkett, Diverse functions of IL-2, IL-15, and IL-7 in lymphoid homeostasis. *Annu. Rev. Immunol.* **24**, 657–679 (2006).
17. P. E. Kovanen, W. J. Leonard, Cytokines and immunodeficiency diseases: Critical roles of the gamma(c)-dependent cytokines interleukins-2, -4, -7, -9, -15, and -21, and their signaling pathways. *Immunol. Rev.* **202**, 67–83 (2004).
18. A. Marçais *et al.*, The metabolic checkpoint kinase mTOR is essential for IL-15 signaling during the development and activation of NK cells. *Nat. Immunol.* **15**, 749–757 (2014).
19. O. M. Anton, S. Vielkind, M. E. Peterson, Y. Tagaya, E. O. Long, NK cell proliferation induced by IL-15 trans-presentation is negatively regulated by inhibitory receptors. *J. Immunol.* **195**, 4810–4821 (2015).
20. F. Brilot, T. Strowig, S. M. Roberts, F. Arrey, C. Münz, NK cell survival mediated through the regulatory synapse with human DCs requires IL-15Ralpha. *J. Clin. Invest.* **117**, 3316–3329 (2007).
21. R. Barreira da Silva, C. Graf, C. Münz, Cytoskeletal stabilization of inhibitory interactions in immunologic synapses of mature human dendritic cells with natural killer cells. *Blood* **118**, 6487–6498 (2011).
22. R. Barreira da Silva, C. Münz, Natural killer cell activation by dendritic cells: Balancing inhibitory and activating signals. *Cell. Mol. Life Sci.* **68**, 3505–3518 (2011).
23. C. Bergamaschi *et al.*, Circulating IL-15 exists as heterodimeric complex with soluble IL-15Rα in human and mouse serum. *Blood* **120**, e1–e8 (2012).
24. E. Mortier, J. Bernard, A. Plet, Y. Jacques, Natural, proteolytic release of a soluble form of human IL-15 receptor alpha-chain that behaves as a specific, high affinity IL-15 antagonist. *J. Immunol.* **173**, 1681–1688 (2004).
25. F. Tamzalit *et al.*, IL-15.IL-15Rα complex shedding following trans-presentation is essential for the survival of IL-15 responding NK and T cells. *Proc. Natl. Acad. Sci. U.S.A.* **111**, 8565–8570 (2014).
26. N. Martínez-Martín *et al.*, T cell receptor internalization from the immunological synapse is mediated by TC21 and RhoG GTPase-dependent phagocytosis. *Immunity* **35**, 208–222 (2011).
27. A. M. Ring *et al.*, Mechanistic and structural insight into the functional dichotomy between IL-2 and IL-15. *Nat. Immunol.* **13**, 1187–1195 (2012).
28. L. M. Costantini *et al.*, A palette of fluorescent proteins optimized for diverse cellular environments. *Nat. Commun.* **6**, 7670 (2015).
29. M. L. Markwardt *et al.*, An improved cerulean fluorescent protein with enhanced brightness and reduced reversible photoswitching. *PLoS One* **6**, e17896 (2011).
30. S. Viaud *et al.*, Dendritic cell-derived exosomes promote natural killer cell activation and proliferation: A role for NKG2D ligands and IL-15Ralpha. *PLoS One* **4**, e4942 (2009).
31. T. W. Hand *et al.*, Differential effects of STAT5 and PI3K/AKT signaling on effector and memory CD8 T-cell survival. *Proc. Natl. Acad. Sci. U.S.A.* **107**, 16601–16606 (2010).
32. M. Merkenschlager, A. Marcais, microRNAs calibrate T cell responses by regulating mTOR. *Oncotarget* **6**, 34059–34060 (2015).
33. D. G. Osborne, S. A. Wetzel, Trogocytosis results in sustained intracellular signaling in CD4(+) T cells. *J. Immunol.* **189**, 4728–4739 (2012).
34. M. E. Dudley *et al.*, Adoptive cell therapy for patients with metastatic melanoma: Evaluation of intensive myeloablative chemoradiation preparative regimens. *J. Clin. Oncol.* **26**, 5233–5239 (2008).
35. E. F. Castillo, S. W. Stonier, L. Frasca, K. S. Schluns, Dendritic cells support the in vivo development and maintenance of NK cells via IL-15 trans-presentation. *J. Immunol.* **183**, 4948–4956 (2009).
36. J. C. Rieckmann *et al.*, Social network architecture of human immune cells unveiled by quantitative proteomics. *Nat. Immunol.* **18**, 583–593 (2017).
37. V. Duprez, A. Dautry-Varsat, Receptor-mediated endocytosis of interleukin 2 in a human tumor T cell line: Degradation of interleukin 2 and evidence for the absence of recycling of interleukin receptors. *J. Biol. Chem.* **261**, 15450–15454 (1986).
38. T. R. Malek, I. Castro, Interleukin-2 receptor signaling: At the interface between tolerance and immunity. *Immunity* **33**, 153–165 (2010).
39. A. Yu, F. Olosz, C. Y. Choi, T. R. Malek, Efficient internalization of IL-2 depends on the distal portion of the cytoplasmic tail of the IL-2R common gamma-chain and a lymphoid cell environment. *J. Immunol.* **165**, 2556–2562 (2000).
40. R. Villaseñor, Y. Kalaidzidis, M. Zerial, Signal processing by the endosomal system. *Curr. Opin. Cell Biol.* **39**, 53–60 (2016).
41. Y. Shimizu, R. DeMars, Production of human cells expressing individual transferred HLA-A,-B,-C genes using an HLA-A, -B, -C null human cell line. *J. Immunol.* **142**, 3320–3328 (1989).
42. P. Delgado *et al.*, Essential function for the GTPase TC21 in homeostatic antigen receptor signaling. *Nat. Immunol.* **10**, 880–888 (2009).